Aerodynamic Parameters Estimated from Flight and Wind Tunnel Data

V. Klein*
Joint Institute for Advancement of Flight Services, George Washington University
NASA Langley Research Center, Hampton, Virginia
and
J.G. Batterson†
NASA Langley Research Center, Hampton, Virginia

A procedure for determination of aerodynamic model structure and estimation of aerodynamic parameters is applied to data from a modern fighter operating within an angle of attack range of 5-60 deg. The paper briefly describes the airplane, available flight and wind tunnel data, postulated models for airplane aerodynamic coefficients, and flight data analysis. The results presented contain only a small number of selected longitudinal and lateral parameters. These parameters were obtained from various maneuvers and subsets of joined data from several flights. The estimated parameters are in good agreement with the wind tunnel measurements. The resulting aerodynamic model equations seem to be satisfactory for the prediction of airplane motion.

Nomenclature

b = wing span, m
$\bar{c}$ = mean aerodynamic chord, m
C_a = general aerodynamic force and moment coefficient
$C_{\ell,m,n}$ = rolling, pitching, and yawing moment coefficients, respectively
$C_{Y,Z}$ = lateral and vertical force coefficients, respectively
p,q,r = roll rate, pitch rate, and yaw rate, respectively, rad/s or deg/s
V = airspeed, m/s
α = angle of attack, rad or deg
β = angle of sideslip, rad or deg
θ = pitch angle, rad
$\delta_{d,h,r}$ = differential tail, symmetric tail, and rudder deflection, respectively, rad or deg

Aerodynamic derivatives are referenced to a system of body axes with the origin at the airplane center of gravity, as

$$C_{a_p}=\frac{\partial C_a}{\partial(pb/2V)},\quad C_{a_r}=\frac{\partial C_a}{\partial(rb/2V)},\quad C_{a_\beta}=\frac{\partial C_a}{\partial\beta}$$

$$C_{a_{\delta d}}=\frac{\partial C_a}{\partial\delta_d},\quad C_{a_{\delta r}}=\frac{\partial C_a}{\partial\delta_r}\quad (a=Y,Z,\ell,m,\text{ or } n)$$

$$C_{a_{\beta\delta h}}=\frac{\partial^2 C_a}{\partial\beta\partial\delta_h},\quad C_{a_{\delta d\delta h}}=\frac{\partial^2 C_a}{\partial\delta_d\partial\delta_h}\quad (a=Y,\ell,\text{ or } n)$$

$$C_{a_q}=\frac{\partial C_a}{\partial(q\bar{c}/2V)},\quad C_{a_{\beta 2}}=\frac{1}{2}\,\frac{\partial^2 C_a}{\partial\beta^2},$$

$$C_{a_{\beta^2\alpha}}=\frac{1}{2}\,\frac{\partial\beta^2\partial\alpha}{\partial^3 C_a},\quad C_{a_{\delta h}}=\frac{\partial C_a}{\partial\delta_h}\quad (a=Z\text{ or } m)$$

Received March 17, 1985; revision received Oct. 25, 1985.

*Research Professor. Associate Fellow AIAA.

†Aerospace Technologist.

Introduction

A procedure for the determination of airplane model structure and parameters from flight data has been developed in Refs. 1 and 2 and later reported in Ref. 3. The procedure is implemented by using stepwise regression and several decision criteria that allow for the selection of an adequate model from postulated terms in the aerodynamic model equations. These equations are based either on polynomials in airplane response and input variables or on polynomial splines approximating the aerodynamic functions. The above technique for airplane model structure determination was successfully applied to pre- and poststall data of a general aviation airplane in Refs. 1 and 2.

The main purpose of this paper is to demonstrate the extension of the technique mentioned to a different class of airplanes by presenting the results of applying the technique to data from a modern fighter airplane. Some of the preliminary results have already been published in Ref. 4. In this paper, new results based on additional flight measurements and revised data analysis are included.

The flight data available for the analysis can be divided into three groups: the small-amplitude longitudinal and lateral maneuvers, large-amplitude maneuvers, and quasisteady deceleration-acceleration maneuvers. All estimated aerodynamic parameters and functions selected for presentation in this paper are compared with the results of the wind tunnel measurements. Finally, the prediction capability of the model determined from flight data is illustrated in an example.

Airplane

The airplane is a twin-engine, high-performance fighter with variable wing sweep. A top view line drawing is given in Fig. 1. The left and right horizontal stabilator act both symmetrically and differentially, providing pitch and roll control, respectively. The average setting of the stabilator provides the pitch control. At low speeds, spoilers on the wing are used for additional roll control. The rudders on the twin vertical tails provide control in yaw. The test configuration consisted of the wing in the 21 deg sweep position with full span slats on the outboard panels deflected at 8.5 deg and the trailing-edge flap deflected at 11 deg.

The flight data were obtained in the form of input-output time histories with 50 samples/s. With each set of data, the values of air density; airplane mass, c.g. location; and inertias were provided either at the beginning of each maneuver only (maneuver header) or during the whole maneuver (separate data printout). The data available for the analysis can be divided into three groups: small-amplitude longitudinal and lateral maneuvers, large-amplitude transient maneuvers, and deceleration-acceleration maneuvers.

The small-amplitude maneuvers were specifically designed for airplane parameter estimation. They were initiated from trimmed conditions at several values of α_{trim} between 5 and 40 deg. The inputs were in the form of either pulses or doublets. In some cases, the inputs were of such small amplitude and/or short duration that they caused insufficient excitation of airplane responses. Although spoilers are normally active, some of the lateral maneuvers were performed with spoilers closed. Examples of the longitudinal and lateral maneuvers will be seen later in a comparison of measured and computed airplane responses.

The large-amplitude transient maneuvers comprised two sets of data. The first set was not intended for model structure determination and parameter estimation. The maneuvers were flown for the evaluation of stability and handling characteristics in high α flight regimes. In these maneuvers, the motion consisted of predominantly lateral modes with α changing from 0 to 60 deg and β sometimes exceeding 25 deg. The time histories indicated that the large-amplitude manuevers contained some possible deficiencies for use in airplane identification. For example, during these maneuvers, all airplane modes were not persistently excited because of the small variation in the differential tail and rudder deflection. Very often, the maneuvers started with rapid changes in α, θ, and V, but only small variations in the remaining output variables. For these reasons, the data from 19 maneuvers were joined together into one set of data. The resulting ensemble of about 9000 data points was partitioned into 23 subsets according to the values of α (see Ref. 2 or 5 for an explanation of the partitioning procedure and its impact on model simplification). A histogram summarizing the number of data points in each subset is given in Fig. 2, where the width of each rectangle represents the width of the corresponding subset and the height corresponds to the number of points in that subset. For the new sets of data, the lateral coefficients were modeled primarily on 2 deg subspaces of the 0-60 deg α space.

In contrast to the first set of large-amplitude maneuvers, the second set was flown explicitly for parameter estimation. This second set of large-amplitude data was comprised of five longitudinal and four combined (longitudinal and lateral) transient maneuvers. The longitudinal transient data were analyzed first as individual maneuvers and second as an ensemble data set from the five longitudinal maneuvers partitioned according to the values of α and δ_h. First, the data were partitioned into subspaces of the 0-50 deg α space. The four combined maneuvers were used in the form of a partitioned data set only. This set of data was also partitioned into 2 deg subspaces of the 0-50 deg α space.

Finally, the deceleration-acceleration maneuvers were considered quasisteady and analyzed accordingly. A review of all flights from which the various maneuvers were taken is given in Table 1.

Wind Tunnel Measurements

Over several years extensive studies of selected configurations of the test airplane were conducted in various wind tunnels. The data from one set of static tests are presented in Ref. 6. These data were obtained from measurements in the Langley 7×10 ft high-speed tunnel at a Mach number of 0.15 using a 1/16-scale model. The corresponding Reynolds number was 0.61×10^6 based on the wing reference chord. During the test, the angle of attack varied from 0 to 50 deg and sideslip from −20 to 20 deg. Pitch, roll, and yaw control effectiveness were studied as well as the effect of spoilers for the configuration with the wing in the 22 deg sweep position, full span slats on the outboard panels deflected 8.5 deg, and leading-edge flaps deflected 10 deg. All of the measured data were presented without analysis. It was, therefore, necessary to estimate stability and control derivatives and their variation with α and β. Because of the significant effect of the tail-plane setting on the various aerodynamic coefficients, the derivatives were estimated for fixed values of δ_h and for δ_h corresponding to trimmed conditions.

Additional wind tunnel measurements of a 1/16-scale model of the airplane with various stores and control settings were carried out in the 7×10 ft transonic tunnel at the David W. Taylor Naval Ship Research and Development Center. The test of a clean configuration with sweep position at 22 deg and corresponding slat and flap deflections was performed at Mach number 0.7 and Reynolds number 2.8×10^6. Some of the results are included in Ref. 7.

A comprehensive set of oscillatory derivatives was measured in the low-speed 30×60 ft tunnel at Langley using a 1/10-scale model. The measurement was conducted at a Reynolds number of about 0.4×10^6. Tests were made for sweep angles of 22, 30, 50, and 68 deg with the slats and flaps retracted. The results of these measurements are given in Ref. 8. Some unpublished data also include the measurements with both slats and flaps deflected.

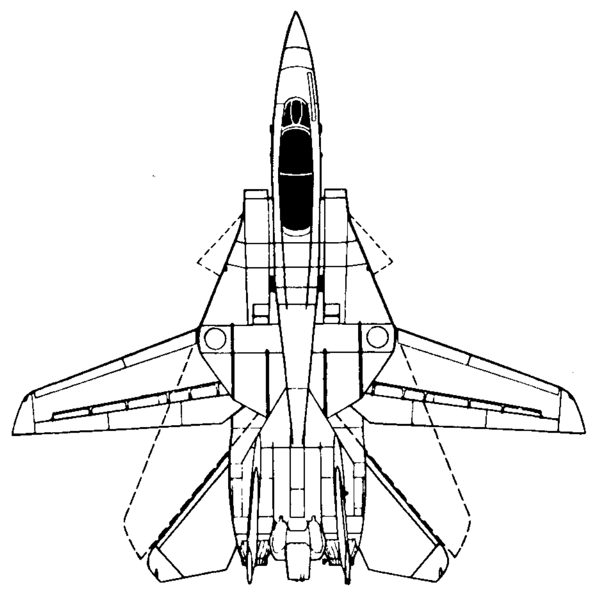

Fig. 1 Top view line drawing of test airplane.

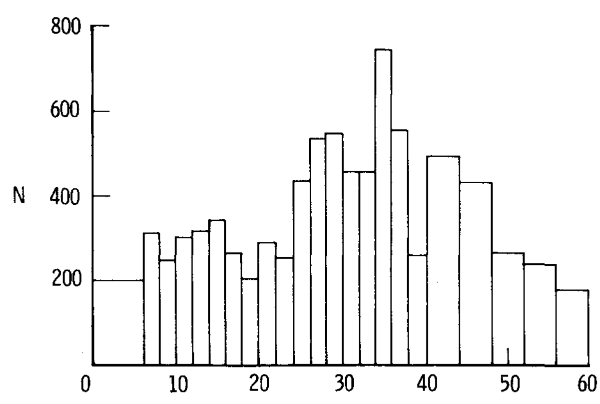

Fig. 2 Number of data points in subsets using partitioning of data from large-amplitude maneuvers.

Table 1 Review of flights that provided data for airplane identification and parameter estimation

Flight	Data group	Comments
331,332 354,355 357,375	I	Small-amplitude maneuvers. Analyzed as small-perturbation transient maneuvers
474,478	II, set 1	Large-amplitude maneuvers for verification of simulation studies. Not designed for parameter estimation. Analyzed by combining all data and partitioning into subsets on α space
562,563	II, set 2	Large-amplitude maneuvers specifically designed for parameter estimation. Analyzed as individual maneuvers and by combining and partitioning data on α and δ_h space
562,563	III	Deceleration-acceleration maneuvers. Analyzed as a quasisteady maneuver for estimation of pitching moment and lift curve

Postulated Models

The airplane equations of motion were referred to the body axes and used in their general form, see e.g. Ref. 1 or 9. For the small-amplitude maneuvers, the aerodynamic coefficients were postulated as polynomials in input and output variables. These polynomials included the linear terms (stability and control derivatives) and higher-order terms expressing the variations of stability and control derivatives with α and β, see Ref. 1.

For the large-amplitude maneuvers, the polynomial splines in α and β were used in the postulated aerodynamic functions. The longitudinal aerodynamic coefficients were approximated as

$$C_a(\alpha,q,\delta_h) = C_a(\alpha)_{\delta h = -15\ \mathrm{deg}} + C_{a_q}(\alpha)\frac{q\bar{c}}{2V} + C_{a\delta h}\Delta\delta_h \tag{1}$$

$$(a = Z \text{ or } m)$$

where $\Delta\delta_h = \delta_h + 0.26178$ rad (15 deg). The terms on the right-hand side of Eq. (1) represent splines in α. A polynomial spline of degree m with continuous derivatives up to degree $m-1$ approximating a function for $\alpha\epsilon(\alpha_0,\alpha_{\max})$ can be written as

$$S_m(\alpha) = \sum_{h=0}^{m} C_h\alpha^h + \sum_{i=1}^{k} D_i(\alpha-\alpha_i)_+^m \tag{2}$$

where

$$(\alpha-\alpha_i)_+^m = 0 \text{ for } \alpha<\alpha_i$$

$$= (\alpha-\alpha_i)^m \text{ for } \alpha \geq \alpha_i$$

The values of $\alpha_1, \alpha_2, \ldots, \alpha_k$ are knots that are ordered as $\alpha_0 < \alpha_1 < \ldots \alpha_k < \alpha_{\max}$ and C_h and D_i are constant coefficients. This form of the spline is chosen based on experience as reported in Ref. 10.

In Eq. (1), no $\dot{\alpha}$ term is explicitly introduced because of the near-linear dependence of $\dot{\alpha}$ on the remaining variables. The effect of $\dot{\alpha}$ is included primarily in contribution due to pitching velocity. Also not included in Eq. (1) are variables that might express a possible aerodynamic coupling. The reasons for the omission of these terms were the relatively small lateral motion during the large-amplitude longitudinal maneuvers and an attempt to keep the model as simple as possible. Derivatives expressing "change with α," such as C_{a_α}, are not included because the partitions assume a small $\Delta\alpha$ for each subset. The lateral coupling terms were, however, included in models using partitioned data. For the data partitioned with respect to α, the aerodynamic model equations were expressed as

$$C_a(\bar{\alpha}, q, \delta_h, \beta, p, r, \delta_d, \delta_r)$$

$$= C_a(\bar{\alpha}) + C_{a_q}\frac{q\bar{c}}{2V} + C_{a\delta h}\Delta\delta_h$$

$$+ C_{a_\beta}|\beta| + C_{a_{\beta^2}}\beta^2 + \sum_{i=1}^{k} C_{a_{\beta i}^2}(|\beta|-\beta_i)_+^2$$

$$+ C_{a_p}\left|\frac{pb}{2V}\right| + C_{a_r}\left|\frac{rb}{2V}\right| + C_{a\delta d}|\delta_d| + C_{a\delta r}|\delta_r|; \ (a = Z \text{ or } m) \tag{3}$$

where $\bar{\alpha}$ denotes the midpoint of an α interval, $\beta_i > 0$ are knots, and

$$(|\beta|-\beta_i)_+^2 = 0 \text{ for } |\beta| < \beta_i$$

$$= (|\beta|-\beta_i)^2 \text{ for } |\beta| \geq \beta_i$$

For the data partitioned with respect to δ_h the model was changed as

$$C_a(\bar{\delta}_h, \alpha, q, \beta, p, r, \delta_d, \delta_r)$$

$$= C_a(\bar{\delta}_h) + C_a(\alpha)_{\delta h = \bar{\delta} h} + C_{a_q}(\alpha)\frac{q\bar{c}}{2V}$$

$$+ C_{a_\beta}|\beta| + C_{a_{\beta^2}}\beta^2 + C_{a_{\beta^2\alpha}}\beta^2\alpha$$

$$+ C_{a_p}\left|\frac{pb}{2V}\right| + C_{a_r}\left|\frac{rb}{2V}\right| + C_{a\delta d}|\delta_d|$$

$$+ C_{a\delta r}|\delta_r|; \quad (a = Z \text{ or } m) \tag{4}$$

The approximation for the lateral aerodynamic coefficients in combined maneuvers is given in Ref. 3.

For the α-partitioned data, the model was used in the form

$$C_a(\bar{\alpha}, \beta, p, r, \delta_d, \delta_h, \delta_r)$$
$$= C_a(\bar{\alpha}) + C_{a\beta}\beta + \sum_{i=1}^{k} C_{a\beta i}\beta\left(1 - \frac{\beta_i}{\beta}\right)_+$$
$$+ C_{a_p}\frac{pb}{2V} + C_{a_r}\frac{rb}{2V} + C_{a\delta d}\delta_d$$
$$+ C_{a\delta r}\delta_r + C_{a\beta\delta h}\beta\delta_h + C_{a\delta d\delta h}\delta_d\delta_h$$
$$(a = Y, \ell, \text{ or } n) \tag{5}$$

where

$$\beta(1-\beta_i/\beta)_+ = 0 \text{ for } |\beta| < \beta_i$$
$$= \beta - \beta_i \text{ for } \beta \geq \beta_i$$
$$= \beta + \beta_i \text{ for } \beta \leq -\beta_i$$

The value of β_i is always taken as positive by convention, which means that $C_a(\beta)$ is assumed to be an odd function. The last two terms in Eq. (5) include the effect of symmetric stabilator deflection (tailplane setting) on lateral parameters. These two terms were included on the basis of wind tunnel measurements.

Flight Data Analysis

All of the data from the transient maneuvers were analyzed using a stepwise regression (SR). As a modified version of the linear regression, this method can determine the structure of aerodynamic model equations and estimate the model parameters. The determination of an adequate model for the aerodynamic coefficients includes three steps: the postulation of terms that might enter the model, selection of an adequate model, and the verification of the model selected. As shown in the previous section, the general form of aerodynamic model equations can be written as

$$y(t) = \theta_0 + \theta_1 x_1(t) \ldots + \theta_n x_n(t) \tag{6}$$

where $y(t)$ represents the resultant coefficient of aerodynamic force or moment. In the polynomial representation of the aerodynamic coefficient, θ_1 to θ_n are the stability and control derivatives, θ_0 is the value of any particular coefficient corresponding to the initial steady-flight conditions, and x_1 to x_n are the airplane output and control variables or their combinations. If splines are used in Eq. (6), then θ_0 to θ_n are the constants in the spline approximation of the aerodynamic functions.

After postulating the aerodynamic model equations, the determination of significant terms among the candidate variables and estimation of the corresponding parameters follows. The variable chosen for entry into the regression equation is the one that has the largest correlation with y after adjusting for the effect on y of the variables already selected. The parameters are estimated by minimizing the cost function

$$J_{\text{SR}} = \sum_{i=1}^{N} [y(i) - \theta_0 - \sum_{j=1}^{\ell} \theta_j x_j(i)]^2$$

where N is the number of data points and $(\ell + 1)$ the number of parameters in the regression equation.

At every step of the regression, the variables incorporated into the model in previous stages and a new variable entering the model are re-examined. Any variable that provides a nonsignificant contribution (due to correlation with more recently added terms) is removed from the model. The process of selecting and checking variables continues until no more variables are admitted to the equation and no more are rejected. Experience shows, however, that the model based only on the significance of individual parameters in model Eq. (6) can still include too many terms and therefore may have poor prediction capabilities. Several criteria for the selection of an adequate model are introduced in Ref. 1 and the details of the whole procedure are explained in Refs. 1 and 2.

A limited number of small-amplitude maneuvers were also analyzed by the maximum likelihood (ML) method of Ref. 9, assuming no external noise and using the model structure determined by stepwise regression. The corresponding cost function has the form

$$J_{\text{ML}} = \sum_{i=1}^{N} \sum_{j=1}^{m} \frac{1}{\hat{\sigma}_j^2} [z_j(i) - \hat{z}_j(i, \hat{\theta})]^2$$

where m is the number of output variables, $\hat{\sigma}^2$ the variance estimate of measurement noise, z_j and $\hat{z}_j$ the measured and computed outputs, respectively, and $\hat{\theta}$ the estimates of unknown parameters.

Discussion of Results

The longitudinal parameters presented in this paper include the pitching moment coefficient C_m and damping in pitch parameter C_{m_q}. The variation of C_m with α was determined from a deceleration-acceleration run and from large-amplitude maneuvers using partitioned data and data from single maneuvers. The results from flight data are referred to

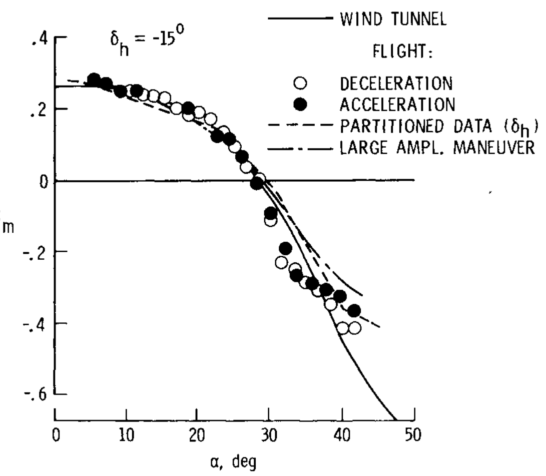

Fig. 3 Comparison of pitching moment coefficient in steady-state conditions estimated from flight and measured in wind tunnel.

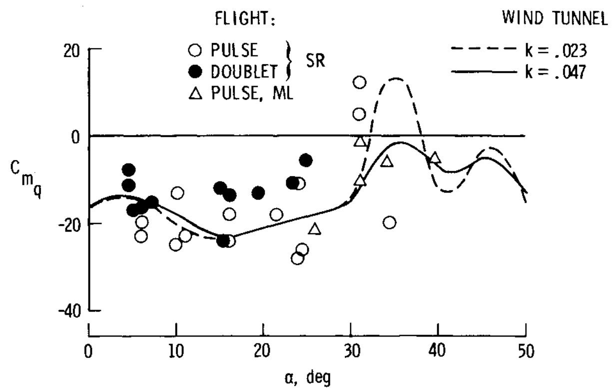

Fig. 4 Comparison of damping-in-pitch parameter estimated from small-amplitude maneuvers and wind tunnel measurement.

as $\delta_h = -15$ deg and are compared with wind tunnel measurements at the same stabilator deflection in Fig. 3. All of the data presented agree very well for α of 5-28 deg. Differences in various results appear at $\alpha > 30$ deg, which is the region where the $C_L(\alpha)$ curve first reaches its maximum (around 32 deg) and then starts decreasing due to flow separation over the whole wing; see Refs. 6 and 8. For $\alpha > 40$ deg, the flight results indicate a tendency for much smaller C_m than that obtained from the wind tunnel. This disagreement could be attributed to different Reynolds numbers during wind tunnel ($Re = 6 \times 10^6$) and flight ($Re \doteq 30 \times 10^6$) testing.

Figures 4 and 5 contain the estimates of C_{m_q} from flight and wind tunnel measurements. The small-amplitude maneuvers used for these estimates were excited by stabilator deflection in the form of a simple pulse or doublet. The results from runs with doublet inputs are close to the estimates from large-amplitude maneuvers in Fig. 5. In this figure, three different flight results are given, namely, the estimates from a single maneuver and from data partitioned with respect to α and δ_h. In the prestall region, these results agree quite well. For higher α, the second set of partitioned data could not predict any variation of C_{m_q} with α. This insensitivity to possible α variation and the scatter in the flight results can be caused by reduced identifiability of C_{m_q}, which is especially noticeable in the poststall region. In the prestall region, the wind tunnel gives greater values of the parameter than the flight data. The different Reynolds number and configuration for flight and wind tunnel test could contribute to this discrepancy. The wind tunnel test for C_{m_q} was conducted with flaps and slats retracted.

The remaining estimates from transient maneuvers presented in this paper contain the derivatives of rolling and yawing moment coefficients. The estimation of these parameters involved some identifiability problems, mainly due to the following: the test data exhibited either small excitation of the yawing motion (small-amplitude and the second set of large-amplitude maneuvers) or rather benign variations in the yawing velocity (first set of large-amplitude maneuvers). Then, the wind tunnel data show rapid changes in parameters C_{n_β} and C_{ℓ_p} with α and, at the same time, small values of these parameters within certain regions of α.

The estimates of directional stability parameter C_{n_β} are given in Figs. 6 and 7. It is shown in Fig. 6 that values from both estimation techniques, that is SR and ML, agree well with the wind tunnel prediction for $\alpha > 10$ deg. In the region of $\alpha < 10$ deg, the parameter values from the linear regression are smaller than those obtained by the ML method or from the wind tunnel measurements. This discrepancy could be caused by the poor form of the input variables and by an attempt to estimate all parameters in Eq. (6) by the SR method. The ML estimates were obtained with some parameters fixed.

The parameter values of C_{n_β} estimated from two sets of large-amplitude maneuvers are presented in Fig. 7. These estimates correspond to β between ± 5 deg and are referred to $\delta_h = 0$ deg. The effect of δ_h on C_{n_β} is apparent by comparison of wind tunnel data and flight results in Figs. 6 ($\delta_h = \delta_{h\text{trim}}$) and 7 ($\delta_h = 0$ deg). In addition the effect of different test conditions on wind tunnel values is seen in Fig. 7. The estimates from large-amplitude maneuvers agree reasonably well with the wind tunnel data for α of 10-40 deg. The scatter in the estimates for $\alpha > 40$ deg can be caused by poststall flight conditions.

The differential tail effectiveness estimated from small- and large-amplitude maneuvers is presented in Figs. 8 and 9. The wind tunnel data in those figures show only a small effect of δ_h on the parameter $C_{\ell_{\delta d}}$. On the other hand, the secondary effect of differential tail deflection $C_{n_{\delta d}}$ is significantly affected by stabilator setting δ_h. In Fig. 8, the flight and wind tunnel values of $C_{\ell_{\delta d}}$ and $C_{n_{\delta d}}$ are given for trimmed conditions with the spoiler both on and off. All

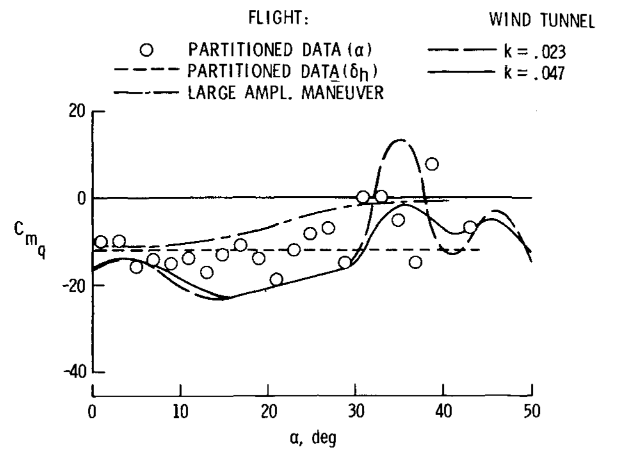

Fig. 5 Comparison of damping-in-pitch parameter estimated from large-amplitude maneuvers and wind tunnel measurement.

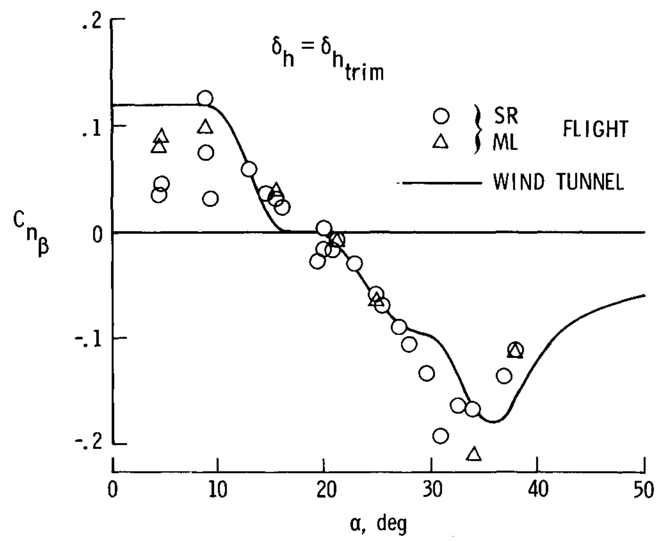

Fig. 6 Comparison of directional stability parameter estimated from small-amplitude maneuvers and wind tunnel measurement.

results agree well. They indicate no contribution of spoiler deflection for $\alpha > 15$ deg and the negative yawing moment due to δ_d.

The estimates of $C_{\ell_{\delta d}}$ for $\delta_h = 0$ are similar to those for trimmed conditions. The small parameter values for low α are the results of limited roll maneuvering and flying some of the maneuvers with the spoiler off. The estimates of $C_{n_{\delta d}}$ for $\delta_h = 0$ deg are, however, different from those in Fig. 8. The negative yawing moment for small values of α becomes adverse for $\alpha > 20$ deg. The parameter $C_{n_{\delta d \delta h}}$, which defines the variation of the $C_{n_{\delta d}}$ with tailplane setting, was estimated from partitioned data and is compared with wind tunnel data in Fig. 10. Both estimates are very close.

The values of damping-in-roll parameter C_{ℓ_p} are plotted vs α in Figs. 11 and 12. The results from small-amplitude maneuvers are close to the wind tunnel measurements within the whole range of α. The results from the two sets of partitioned data exhibit some inconsistency for $\alpha > 20$ deg. This could be caused by different flight conditions and types of maneuvers. The first set of data included various maneuvers with the rolling velocity sometimes reaching 100 deg/s. The maneuvers included in the second set of partitioned data were mostly oscillatory with rolling velocity within ± 30 deg/s range and similar to those used for the estimates in Fig. 11. The results from those two groups of data are quite close.

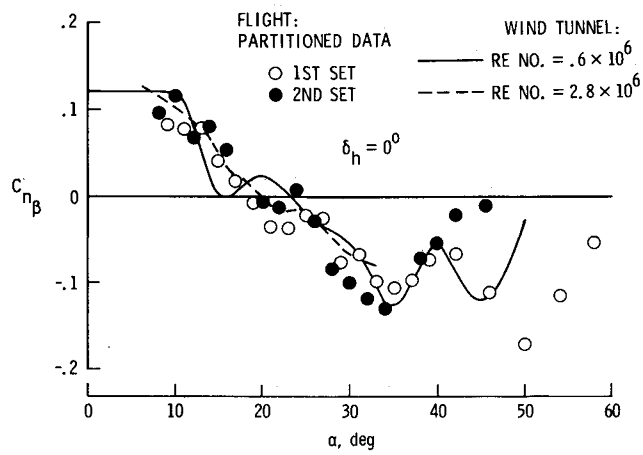

Fig. 7 Comparison of directional stability parameter estimated from large-amplitude maneuvers and wind tunnel measurement.

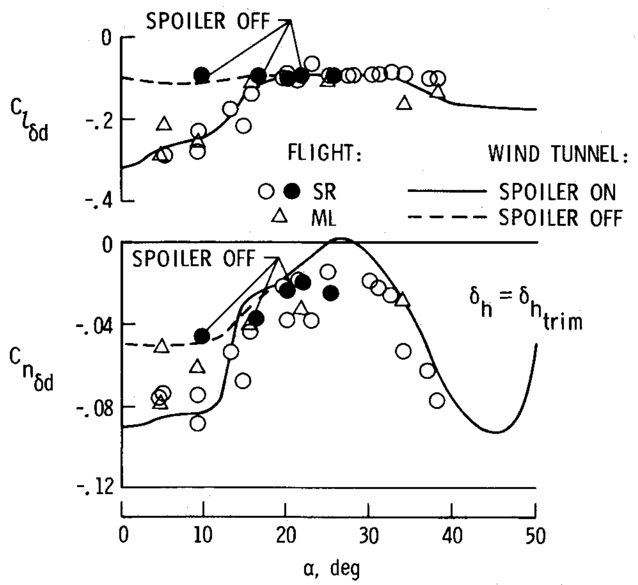

Fig. 8 Comparison of differential tail effectiveness parameters estimated from small-amplitude maneuvers and wind tunnel measurement.

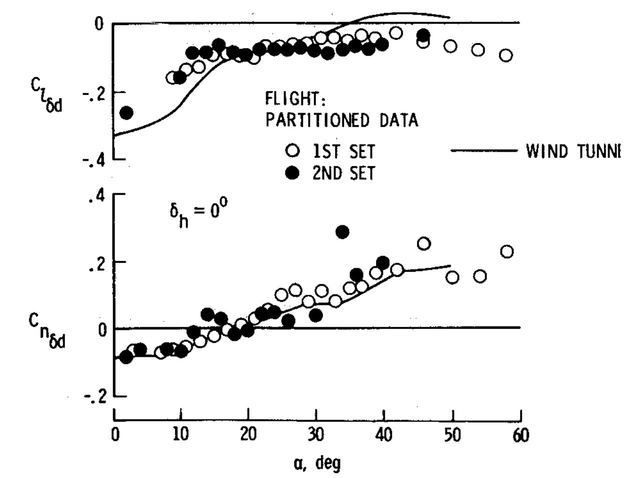

Fig. 9 Comparison of differential tail effectiveness parameters estimated from large-amplitude maneuvers and wind tunnel measurement.

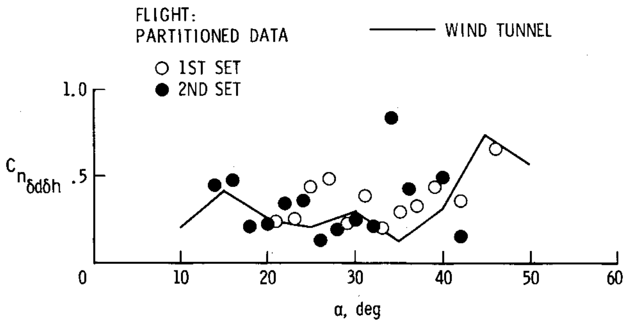

Fig. 10 Comparison of yawing moment due to differential and symmetric tail deflection estimated from large-amplitude maneuvers and wind tunnel measurement.

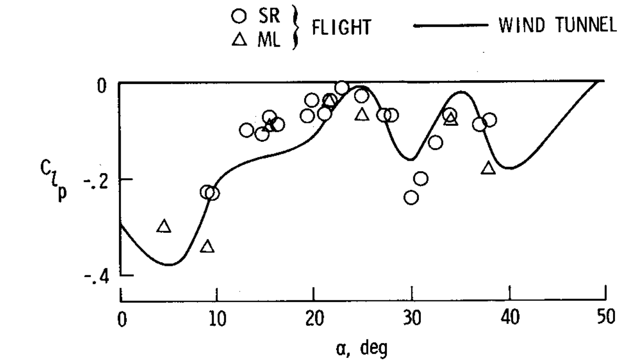

Fig. 11 Comparison of damping-in-roll parameter estimated from small-amplitude maneuvers and wind tunnel measurement.

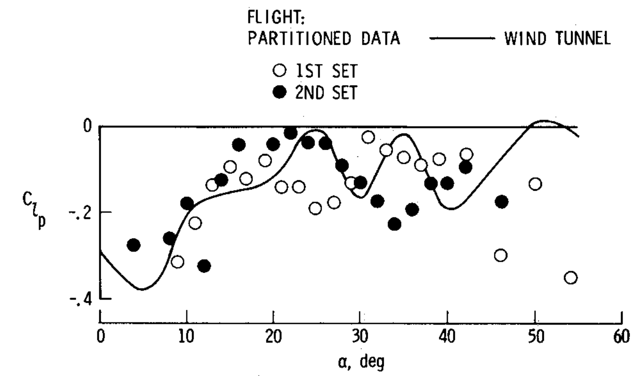

Fig. 12 Comparison of damping-in-roll parameter estimated from large-amplitude maneuvers and wind tunnel measurement.

The estimates of the remaining parameters from the partitioned data were close to the parameters estimated from the small-amplitude maneuvers. The partitioned data did not provide any comprehensive information about nonlinearities of the coefficients with β. For this reason, the results mostly from the partitioned data without these nonlinearities were used in the prediction of the airplane motion. The general equations of motion were integrated using the measured inputs and measured airspeed (the five-degree-of-freedom simulation). One of the results of simulation exhibiting a cross-control maneuver is given in Fig. 13. For most of the time intervals selected, the measured and predicted time histories are similar, thus indicating good prediction capabilities of the model determined from flight data.

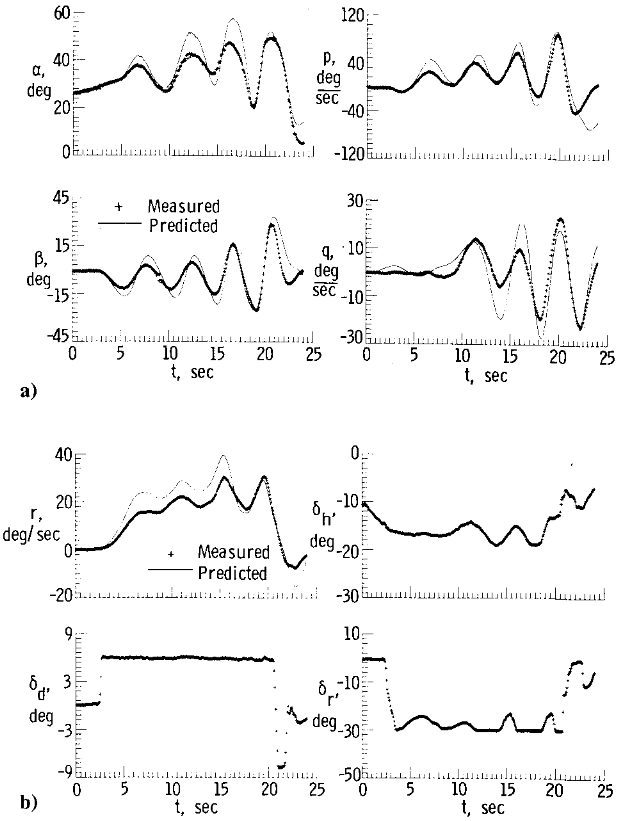

Fig. 13 Measured time histories and those predicted by using parameters obtained from flight data.

Conclusions

A procedure for the estimation of airplane model structure and parameters has been applied to data from a modern fighter airplane operating within the α range of 5-60 deg. The aerodynamic parameters were estimated from small- and large-amplitude transient maneuvers and quasisteady runs. The following conclusions can be drawn from the results reported herein:

1) The small-amplitude maneuvers designed for parameter estimation provided estimates of all stability and control derivatives under trimmed conditions within $5<\alpha<40$ deg. Some inconsistencies in these estimates were mainly caused by insufficient excitation of the airplane motion.

2) The longitudinal maneuvers, transient and quasisteady, provided consistent estimates of pitching moment coefficient and damping in-pitch parameter as functions of α.

3) It was shown that large-amplitude maneuvers, whether or not they were specifically designed for airplane identification, can be used in the analysis of lateral aerodynamics in the form of partitioned data according to the values of α. The partitioned data revealed some interesting details in the aerodynamic model equations, namely the effect of tailplane setting on the yawing moment coefficient.

4) The estimated parameters and functions are in good agreement with the results of static and oscillatory wind tunnel measurements. In addition, the model with estimated parameters from flight data demonstrated good prediction capabilities in small-amplitude maneuvers. Also, reasonably good results were obtained for large-amplitude maneuvers using the five-degree-of-freedom simulation.

The paper presented represents a further step toward the determination of an overall model of the airplane from flight data. The future work should include more emphasis on the design of an experiment, especially the form of input variables. Better experimental data might increase the accuracy of the estimated parameters and provide better knowledge about the aerodynamic model equations within the extended flight envelope. This should be followed by an intensive effort to simulate various six-degree-of-freedom maneuvers within the flight envelope considered.

Acknowledgment

The completion of this research was made possible through the participation and assistance of many people. The authors wish to express their sincere gratitude and appreciation to Mr. F. Schaefer from Grumman Aerospace Corp., Messrs. R.J. Wilson and E.K. Enevoldson from NASA Ames/Dryden, and Mr. R.A. Hess from George Washington University.

References

[1]Klein, V., Batterson, J.G., and Murphy, P.C., "Determination of Airplane Model Structure From Flight Data by Using Modified Stepwise Regression," NASA TP-1916, Oct. 1981.

[2]Klein, V. and Batterson, J.G., "Determination of Airplane Model Structure From Flight Data Using Splines and Stepwise Regression," NASA TP-2126, March 1983.

[3]Klein, V. and Batterson, J.G., "Determination of Airplane Parameters From Flight Data at High Angles of Attack," *Proceedings of 13th Congress of the International Council of the Aeronautical Sciences*, Vol. 1, 1982, pp. 467-474.

[4]Klein, V., Abbasy, I., and Batterson, J.G., "Determination of Aerodynamic Parameters of a Fighter Airplane From Flight Data at High Angles of Attack," AIAA Paper 83-2066, Aug. 1983.

[5]Batterson, J.G., "Estimation of Airplane Stability and Control Derivatives from Large Amplitude Longitudinal Maneuvers," NASA TM-83185, 1981.

[6]Huffman, J.K., Fox, C.H. Jr., and Grafton, S.B., "Subsonic Longitudinal and Lateral Directional Static Stability Characteristics of a Variable Sweep Fighter Configuration Employing Various Control Surface Deflections at Angles of Attack of 0° to 50° and Large Sideslip Angles," NASA TM 74050, Nov. 1977.

[7]Bastedo, W., "Test Data Results of NS RDC High Alpha-Beta Speed Wind Tunnel Test of 1/16-Scale Model F-14A," Grumman Aerospace Corp., Bethpage, NY, Rept. A51-335-1-81-02, Feb. 9, 1981.

[8]Grafton, S.B. and Anglin, E.L., "Dynamic Stability Derivatives at Angles of Attack from −5° to 90° for a Variable-Sweep Fighter Configuration with Twin Vertical Tails," NASA TN D-6909, Oct. 1972.

[9]Grove, R.D., Bowles, R.L., and Mayhew, S.C., "A Procedure for Estimating Stability and Control Parameters From Flight Test Data by Using Maximum Likelihood Methods Employing a Real-Time Digital System," NASA TN D-6735, May 1972.

[10]Klein, V., Batterson, J.G., and Smith, P.L., "On the Determination of Airplane Model Structure from Flight Data," *Identification and System Parameter Estimation—Sixth IFAC Symposium*, Vol. 2, edited by G.A. Bekey and G.N. Saridis, Pergamon Press, New York, 1982, pp. 1034-1039.